Available online www.unicrossjournals.com

UNICROSS JOURNAL OF SCIENCE AND TECHNOLOGY, UJOST

RESEARCH ARTICLE VOL. 1(2) SEPTEMBER, 2022 ISSN:2814-2233

Date Accepted: 31st August, 2022 Pages 38-55

EXTRACTION, CHARACTERIZATION AND MOLECULAR MODELING INVESTIGATION ON THE ANTI-NOCICEPTIVE AND ANTI-INFLAMMATORY EFFECT OF *COSTUSAFER*LEAF EXTRACTS

Moses Mbeh Edim[1], Ewona, Igwe Otaba[2] and Fidelis Ebunta Abeng[3]

[1]Department of Chemistry, Cross River University of Technology, Calabar, Nigeria
[2]Physics Department, Cross River University of Technology, Calabar
[3]Material and Computational Chemistry group, Department of Chemistry, Cross River University of Technology, Calabar, Nigeria
Email: Moses.edim@yahoo.com- corresponding author

Abstract

In the last years, the development of drugs for the treatment of inflammation is very fast. It has been estimated by epidemiological studies that the occurrence of inflammation in the community ranges from 13% to 68%. This employs the need for effective methods to reduce the occurrence of the disease. In this research work, DFT methods and in-silico molecular docking simulation approach has been used on different structures for the case study. The theoretical investigations of the synthesized compounds were computed applying density functional theory at the B3LYP/6-311++g(d,p) and UB3PW91/6-311++g (2d,2p) meta hybrid GGA basis sets. The molecular docking approach compares the energy of the binding affinities, posing excellency in the interactions of the studied compounds in the active sites of the receptor molecules, and evaluates it as a potential anti-inflammatory and anti-nociceptive drug molecule using clinical trials. ADME properties were also carried out to show the drug-likeness ability of the structures. The results were within the permissible limit which indicates a good oral behavior of the structures.

Keywords: *Anti-inflammatory, Anti-nociceptive, DFT, Ad-med properties, Molecular docki*

1.0 Introduction

The progression towards the inhibition potency of drugs used for inflammatory diseases has become increasingly apparent and is a global of serious challenge. This is owing to the high prevalence of the occurrence of pathogens that causes infections. Inflammations can be caused by a sudden encounter of offending agents like viruses or bacteria or even toxic chemicals by the body when any of the tissues are damaged [1]. This then results in pain, swelling, bruising, redness, stiffness and damage to otherwise healthy body tissues. Inflammations could be acute or chronic [2]. Acute inflammation is said to occur as a

result of sudden body damage such as a cut on the finger while chronic inflammation is continuous signaling of inflammatory cells even in the absence of external danger such as rheumatoid arthritis and is detected by a pain or tenderness, heat, swelling or an experience of having a flushed skin at the site of the injury. On the other hand, nociception could be said to be a pain arising from actual or threatened non-neural tissue and is as a result of the activation of nociceptors which could be due to a direct harmful stimulus to the ocular surface [3]. This is to say that it is caused by potentially harmful stimuli which could be mechanical, chemical, thermal or physical which is being detected by sensory receptors around the body. This kind of reactions causes a burning sensation that could likely be termed “nociceptive pain”[4]. Injuries that cause nociceptive pain include: bruises, burns, fractures, overused or joint damage such as arthritis or sprains.This leads to messages of pain being sent from the central nervous system to the brain and causes a numb feeling [5]. There is however a correlation between inflammation and nociception. Inflammation is a type of nociceptive pain that results from activations and sensitizations of nociceptors by inflammatory mediators [6]. Recently, a lot of research work has been attributed to the case study.In 2015, Calado, G. P., Lopes, A. J. O., Costa Junior, L. M., Lima, F. D. C. A., Silva, L. A., Pereira, W. S., ... &Nascimento, F. R. [7] investigated on a plant specie known as Chenopodiumambrosioides L. (Amaranthaceae) to analyze it anti-inflammatory and anti-nociceptive responses of the crude hydroalcoholic extract (HCE) of it leaves. The study used Wistar rats which were separated into six groups (n = 24): clean (C), negative control (CTL-), positive control (CTL+), HCE0.5, HCE5 and HCE50. The first group received no intervention. The other groups received an intra-articular injection of sodium monoiodoacetate (MIA) (8 mg/kg) on day 0. After six hours, they were orally treated with saline, Maxicam plus (meloxicam + chondroitin sulfate) and HCE at doses of 0.5 mg/kg, 5 mg/kg and 50 mg/kg, respectively. The study also performed molecular docking to evaluate the compatibility of ascaridole, a monoterpene found in HCE, with the NMDA receptor and after the third day, the HCE reduced knee edema. HCE5 showed less cellular infiltrate in the cartilage and synovium and lower intensities of allodynia from the third day and of hyperalgesia from the seventh day up to the last treatment day. The HCE5 and HCE50 groups improved in forced walking. Muslu, H., Kalaycıoğlu, Z., Erdoğan, T., Gölcü, A., &Erim, F. B.in 2021 [8] did a research on anti-inflammatory drugs. The study reviewed the synthesis and characterization of copper(II), zinc(II), platinum(II) and palladium(II) complexes of Tenoxican TNX by analytical and instrumental techniques (Ultraviolet and visible absorption spectra (UV–Vis), Liquid chromatography–mass spectrometry (LC-MS), Inductively coupled plasma - optical emission

Spectrometry (ICP-OES), Differential thermal analysis-Thermogravimetric analysis (DTA-TG). Fourier-transform infrared (FT-IR) spectra of the complexes were measured and the outcome was supported by DFT computations. The proposed structure of the metal complexes were [Cu(TNX)2], [Zn(TNX)2], [Pt(TNX)2]

and [Pd(TNX)Cl2]. The anti-inflammatory and anti-nociceptive activities of the synthesized complexes compared with the drug were demonstrated in the study for the first time. All metal complexes of the TNX acted more efficiently on the reduction of pro-inflammatory tumor necrosis factor (TNF)-alpha production than that of TNX. The highest anti-inflammatory and anti-nociceptive potential was detected with [Cu(TNX)2]. The receptor-ligand interactions between TNX complexes and TNF-α were revealed by molecular docking calculations.Obafemi, C. A., Adegbite, O. B., Fadare, O. A., Iwalewa, E. O., Omisore, N. O., Sanusi, K., …&Ceylan, Ü. [9] in 2021 also reported a research on Tryptanthrin as a potent natural alkaloid with good vitro pharmacological properties. The study carried out a test on it analgesic and anti-inflammatory activity and the results revealed a dependent inhibition efficiency of tryptanthrin dose on oedema and pain formation in all the models used. The agent also exhibited significant higher effects in its anti-inflammatory and analgesic activities better than positive drugs (aspirin and indomethacin) that arebeing used currently in the treatment and management of acute and chronic forms of pain and inflammatory disorders. Molecular docking approach was also employed to rationalize the action and prediction of the binding affinity of tryptanthrin. The DFT calculations carried out in the study also revealed that tryptanthrin shows a higher antioxidant activity than ascorbic acid which may be improved upon by functionalizing the aromatic core to enhance its solubility in ionic solvents. Some lifestyles like excessive intake of alcohol, chronic stress, smoke, having a high body mass index that falls within the ranges for obesity except for being very muscular, also contributes to inflammation in the body [10]. The use of antibiotics could go a long way in reducing the symptoms caused by inflammatory pathogens thereby making it appear that the antibiotics are working, but if the right diagnosis can be made, better treatments can be considered.

2.0 Experimental

2.1 Sample preparation

The harvested fresh plant sample taken to the laboratory where the leaves were separated from the stem and thoroughly rinsed with distilled air-dried for two weeks, then ground to powdered form and stored in a deciccator.

Extraction methods

The ground plant materials were extracted by a Soxhlet extraction method with ethanol. The extracts were concentrated to a spury residue using a rotary evaporator to give the extracts.

The digital heidolphrota-evaporator was set at 450c under reduced pressure. The rotary evaporator was first rinsed with solvents of different polarity. The sample flask of the rota-evaporator was filled to one-fourth of its capacity with the filtrate (ethanol extract) and was filtered to the rota machine. The flask was held at an angle and rotated rapidly in the heating bath which was maintained at a temperature of 450c. This action spreads the liquid in a film on the wall of the flask and provided a large surface for evaporation. Care was taken to ensure that bumping of the material did not occur by adjusting the knob provided, immediately the first sign of bumping was observed to let some air to enter the sample

flask. The pressure of the Rota-evaporator was maintained at0.01mmHg.

As the solvent vapour passed through the condenser, it condenses and was recovered in a second round-bottom flask – the solvent recovery flask. The two condensers in the well lagged thermos flaskk filled with ice block baths were also monitored to make sure that the extracted solvent did not suck into the pressure pump during the process. After evaporation of ethanol, filtrate (ethanol extract) was observed to be sticky, dark green in color. The mass of the residue was recorded.

2.2 Gas Chromatography-Mass Spectrum Analysis (GC-MS) Gas chromatography analysis was performed using GC-MS SHIMADZU QP 2010, JAPAN gas chromatography 5890-11 with a fused GC column (OV-101) coated with polymethyl silicon (0.25nm x 50m) and the conditions were as follows: Temperature programming from 80-200oC held at 80oC for 1 minute, rate 5oC/min with a sterile wire loop. Each disc was impregnated with 0.2ml of plant extracts. Discs with DSMO (100mg/ml) served as a control.The discs were used after drying them in an incubator for 40oC to remove any trace of solvent. Discs were introduced into the surface of the medium the plates were incubated at 40oC for 24hours to obtain zones of inhibition. The experiments were repeated three times for each extract and the average of these values is seen in Table S1 in the supporting information

2.3 Statistical analysis

All values are expressed as mean ± S.D. Statistical analyses were done by student's t-test. The values of ρ lower than 0.05 were considered significant.

2.1 Computational method

The ground state geometric structures of the compounds have been optimized using B3LYP/6-311++g(d,p) for the complexes(A1, B1 and C1) and UB3PW91/6-311++g (2d,2p) meta hybrid GGA basis sets for complex (D1) using Gaussian 16 [11] and graphical visualization of same was achieved using the Chemcraft software [12]. The Highest Occupied Molecular Orbital (HOMO) and the Lowest Unoccupied Molecular Orbital (LUMO) was calculated at same basis setsto investigate into the reactivity and stability of the modeled compounds. Properties such as Energy calculations, Frequency calculation, Naturalbond orbital (NBO) and Frontier Molecular Orbital (FMO) analysis were all computed with Gaussian09W software [12]. All frontier molecular orbital (HOMO and LUMO) isosurface maps were plotted using the Avogadro molecular editor and visualization software program [13]. Mulliken charge plot was achieved using the Origin program package [14] to determine the distribution in the charge of the molecules and to ascertain the behavior of its spatial arrangement and potencyof being used as a potential anti-inflammatory and anti-nociceptive agent.Absorption, distribution, metabolism and excretion ADME) properties of the optimized structures have been estimated using Molinspiration software [15] to predict the drug-likeness of the structures.Preparation of ligand for Molecular docking studies was performed using the Discovery studio [16] and the 2D visualization of the ligands and results from the docking interactions were

achieved using the same software package and an additional visualization of same was done using the Pymol[17]. The docking conformations with the highest binding energy were highlighted for additional molecular analysis in order to achieve the optimal conformation. The 3D structure of the proteins was downloaded from the RCSB (Research Collaboratory for Structural Bioinformatics) protein data bank (http://www.rcsb.org/pdb/home/home.do) and is presented in Figure 2 and Auto Dock Vina [18] aided in performing the molecular docking studies.

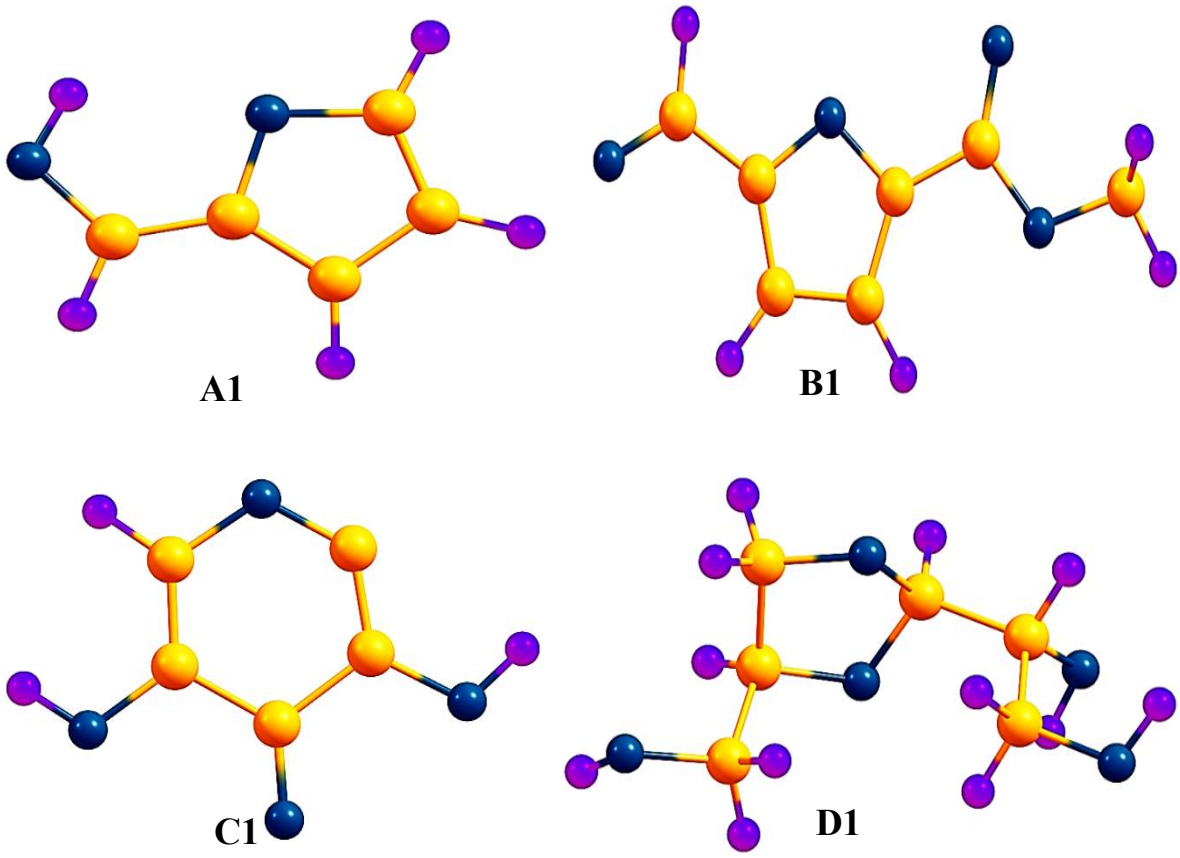

Figure 1: The optimized geometries of the structures A1, B1, C1 and D1

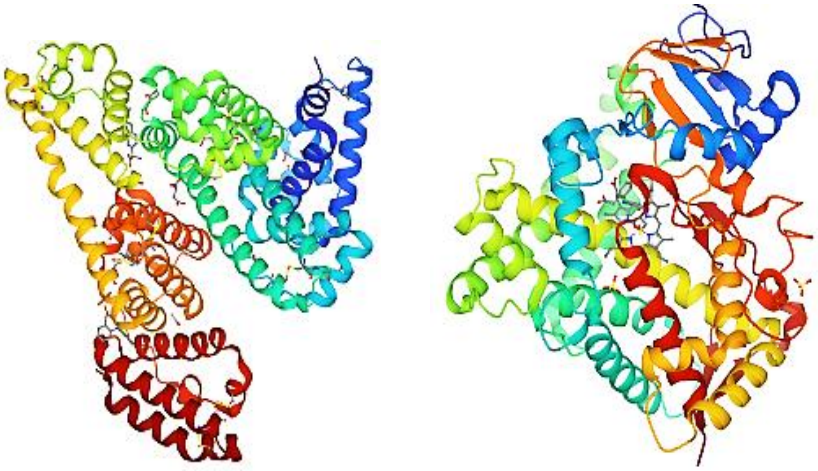

***E. Caballus* (4ZBR)** ***O. Cuniculus* (1NR6)**

Figure 2: 3D structures of the receptor proteins

Results and discussion

3.1 Global reactivity descriptors

For detailed understanding of the various properties exhibited by the isolated compounds, it is important to further study the molecular properties of the isolated compounds based on Koopmans approach [19] to espy the most presumptive and momentous attributes which might facilitate the optimum utilization of A1, B1,C1, and D1 in medicinal field. Global reactivity descriptors like electron affinity (EA), chemical potential (μ), chemical softness (S), ionization potential (IP) and electrophilicity (ω) parameters of the respective complexes were carefully investigated and results reported inTable1. The equation of computation can be found in some of our previous works [20]. However From the results in Table1, higher tendencies of electron or charge transfer will result to an increase in HOMO or IP values, as such A1, B1, C1 and D1complexes has corresponding high HOMO values of -7.425eV, -7.4391eV, -7.2460eV and -7.3117eV respectively which implies that the isolated complex is likely to release electron easily thereby repairing the damaged body tissue and thus acting as a good anti-inflammatory agent which is in tandem with the docking studies. Similarly, the tendency that the investigated complexes would accept electrons is depicted by the lowest unoccupied molecular orbital (LUMO), however a good drug is likely to release electrons easily (highly nucleophilic) than accepting electrons (less electrophilic). Thus, the LUMO value suggests that A1 and B1 complex with -0.00381eV and -2.763eV would not accept electrons easily unlike C1, and D with LUMO values of -18.3241eV and -6.2259eV respectively. It was observed that the IP value of 7.426eV, 7.4391eV, 7.2460eV and 7.3117eV as well as EA of

0.00381eV, 2.763eV, 18.3241eV and 6.2259eV affirms the attributes of A1 and B1 complex as an anti-inflammatoryand anti-nociceptive agent. Nevertheless, the most significant of all parameters listed is the energy gap, as it informs us on whether or not the proposed complex would be stable and less reactive or vice versa, of which the stability of a drug is highly important if it must be efficient and suitable for assimilation. Similarly, an increase in energy gap of the complexes implies that the electronic transition from HOMO to LUMO is not readily assessable, as such reactive specie is considered to have easy transition from one orbital to another with a corresponding minimum amount of energy required (see Figure 3). However, B1 complex can be classified as a stable molecule due to its low energy gap of 4.6761eV compared to A1, C1 and D1 complexes with HOMO-LUMO gap of 7.4254eV, 11.0781eV and 1.0858eV. Thus, from literature report, the lower the energy gap, the higher the stability and less reactivity of the complex [21-23]. Thus this correlate with the docking result obtained as B1 complex was observed to bind effectively with 4ZBR and 1NR6 inflammation receptors with a corresponding bind affinity of -5.8 for both receptors.

Table 1: Global reactivity descriptor values for A1, B1, C1, and D1

Parameters	A1	B1	C1	D1
HOMO/eV	**-7.42500**	**-7.4391**	**-7.2460**	**-7.3117**
LUMO/eV	-0.00381	-2.7630	-18.3241	-6.2259
Eg/eV	7.4254	4.6761	11.0781	1.0858
IP/eV	7.42500	7.4391	7.2460	7.3117
ω(ev)	-25.5709	-30.4182	14.755	-84.235
μ(ev)	-3.7144	-2.338	-0.5439	-0.5439
η(ev)	-3.7105	-5.10105	-6.7687	-6.7687
S(ev)	-0.2692	-0.42771	0.1805	-1.839

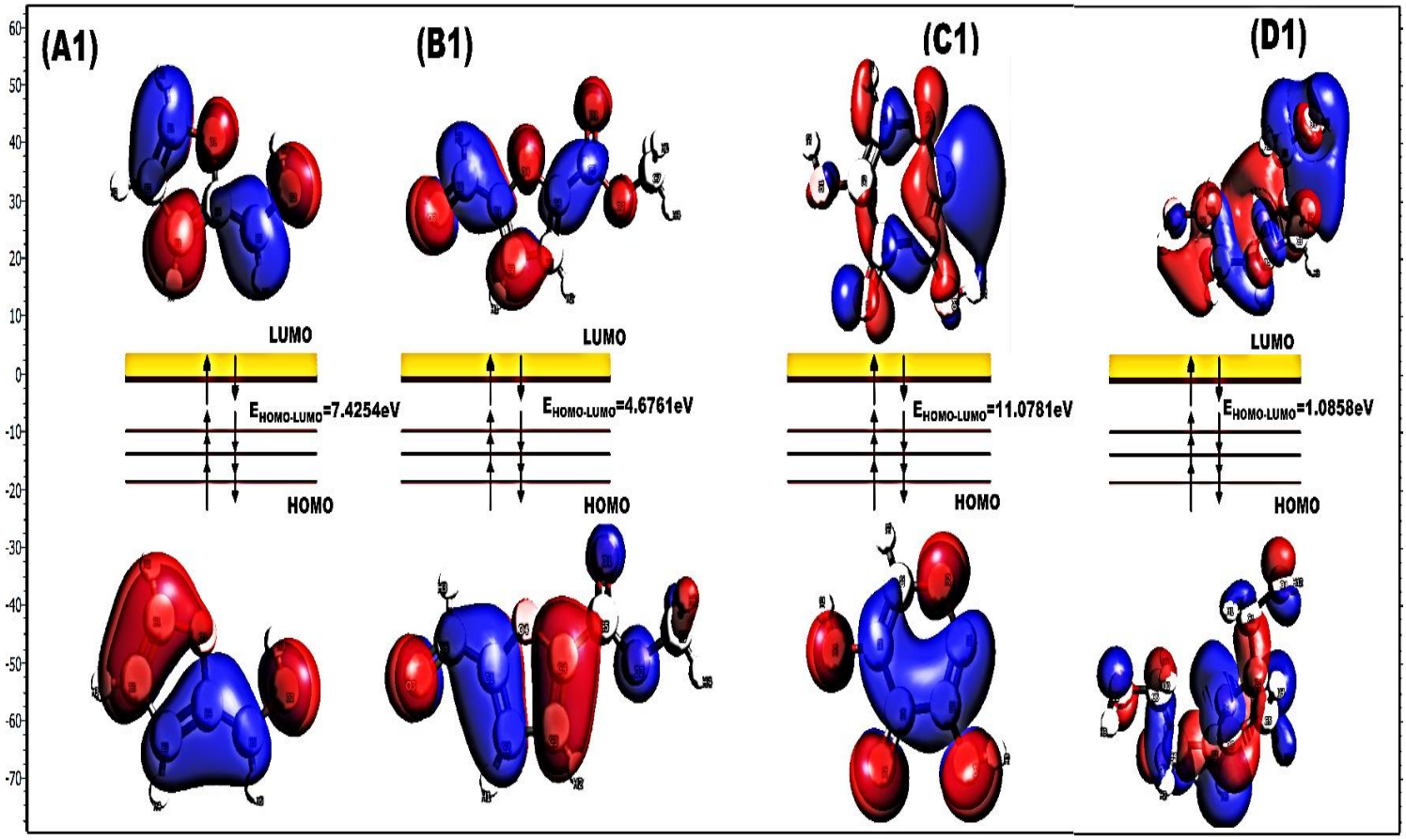

Figure 3: Homo-Lumoiso surface

Appropriate investigation of the natural bonding orbital analysis was carried out to fully grasp the mechanism of charge delocalization within the molecular systems and also to gauge the nature and type of Lewis and non-Lewis's orbital interaction as these will significantly contribute to the stability of the molecules. However, it is important to comprehend with certainty, molecular stability and charge delocalization within the investigated complexes, as such NBO calculation were conducted in gas phase. Also, contributions of resonance structure to molecule, as well as the interaction of anti-bonding and bonding orbitals can be obtained as this knowledge would enhance the efficacious study of the inter-molecular and intra-molecular charge density delocalization and transfer interaction within the isolated complexes. As such it is very crucial to ascertain the strength of the interactions or stabilization enthalpy of each donor and acceptor orbitals. To actualize this, the second perturbation equation;

$$E^{(2)} = \Delta E_{i,j} = -qi\frac{F(i,j)2}{Ei-Ej} \quad (1)$$

was employed [24], where qi represents the total charge density of the donor orbital, $F_{i,j}$designates the off diagonal Fock matrix, E_i-E_j shows the marginal difference in energy term for each donor and acceptor orbitals. The sequitur from the observed interaction in table 3 can be epitomized as thus; the most significant contribution to the stabilization energy of the complexes in gas phase result from charge transfer often associated with charge delocalization which emanate from pi-to-pi bonding to anti-bonding orbital (π→π*), pi to pi antibonding to antibonding orbitals (π*→π*), as well as sigma to sigma bonding to anti-bonding orbitals (σ→σ*). However, the change in charge density transfer (ΔET π→π*) for all complex was calculated to be 14.72kcal/mol, 18.44kcal/mol, for A1 and B1 complexes, whereas the change in charge density transfer (ΔETπ*→π*) for C1 complex is 131.49kcal/mo. Similarly, the results in table 2 reveal that change in charge density transfer (ΔETσ*→σ*) for the investigated complexes are 3.19kcal/mol,7.43kcal/mol for A1 and D1 complexes. Interestingly, it was observed that the interactions are hyperconjugative in nature and the isolated complexes is stabilized by charge transfer emanating mostly from (ΔETπ*→π*), as depicted by the high second perturbation energy $E^{(2)}$ of the investigated compounds from table 3.

Table 3: Second order perturbation theory analysis of fock matrix in NBO basis

Compounds	Donor	Acceptor	E(2) kcal/mol	E(j)-E(i) a.u	F (I,j) a.u
A1	πC1-C2	π*C3-C4	14.72	0.29	0.084
	σC10-H12	σ*C4-O9	3.19	0.87	0.067
B1	πC1-C2	π*C10-O11	18.44	0.29	0.068
	πC3-C4	π*C7-O8	19.61	0.29	0.068
C1	πC1-C2	πC4-O8	71.48	0.01	0.078
	πC4-O8	πC1-C10	60.01	0.01	0.069
D1	σC13-H17	σ*O15-H16	2.71	0.94	0.045
	σC13-H18	σ*C4-O19	4.72	0.80	0.055

3.3 Mulliken Population analysis

Mulliken population charge analysis was conducted to clearly fathom the atomic charges possessed by each atom and to evaluate the effect of functional groups on this charges as well as the distribution of charge density within the isolated systems [25]. Charge density distribution in molecules is very crucial to ascertain the conformational character as well as the efficacy of the isolated system to be used as a potential anti-inflammatory and anti-nociceptive agent. The Mulliken charge of all isolated systems in Figure3 depicts that A1, B1, C1, and D1 complexes have excess electron density of the range ($\approx$-0.14$\rightarrow\approx$-0.49). However, the results clearly elucidate that the specific carbon associated with the hydroxyl group, possess more negative densities than other carbon groups, which results in an uneven electronic distribution within the benzene ring as clearly shown in Figure 3. Also, it was observed that the charge density in C3 = -0.378 for B1 complex, is considerably higher than the charge density observed for other atoms. Similarly, the same is observed for A1, C1 and D1 isolated compounds. The negative charge densities are indicated with red colors, to clearly distinguish the positive and negative charge densities for the isolated systems. Interestingly, it was observed that the corresponding positive charges of the hydrogen atoms for all isolated systems is predisposed by the type and degree of the charge density on carbon counterparts, as clearly depicted by Figure3plot. Thus, the Mulliken population analysis clearly over estimates the charge density of atoms and thus depends strongly on the basis set and functional used, as this is attributed to the sensitivity of Mulliken charge analysis to probability density of the isolated complexes.

Figure 3: Mulliken charge plot

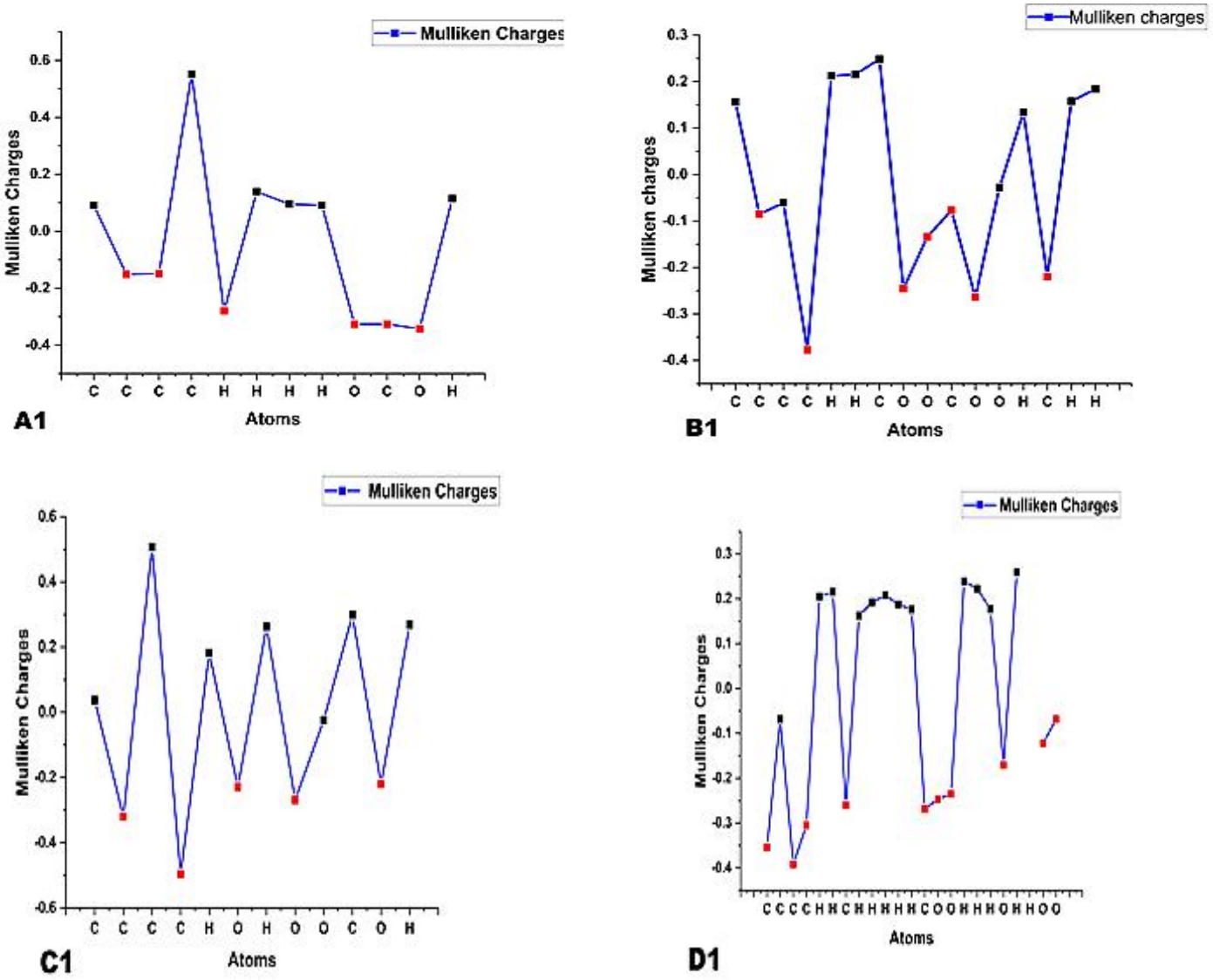

4.0 ADME studies and physiochemical parameters

The ADME (absorption, distribution, metabolism and excretion) properties of the optimized structures have been estimated using Molinspiration software. The predicted topological polar surface area (TPS

A), number of violated drug-likeness rules and Lipinski parameters such as molecular weight (MW), number of rotable bonds (n-rotb), number of hydrogen bond acceptors (n-ON), number of hydrogen bond donors (n-OHNH) and lipophilicity (mLogP) for the complexes is seen in Table 4According to Lipinski's rule [26], molecules with good ADME properties should have no more than one violation (n-Voi) of the following criteria: number of hydrogen bond donors (n-OHNH)< 5, number of hydrogen bond acceptors (n-ON) < 10, lipophilicity (mLogP) < 4.15, molecular weight (MW) < 500. Drug molecules with low molecular weight (<500) can be transported, diffused and absorbed easily compared to drugs with heavy molecules. The optimum values of the descriptors, rotable bonds and polar surface area also contributes greatly on the oral bioavailability for drug molecules. The mLogP values of all the compounds showed excellent permeability across the cell membrane as none was predicted to be more over 4.15. In general, as seen in Table 4 all the studied compounds exhibited no violation of the listed criteria. Hence, they perfectly respect the Lipinski's rule and can be considered as potential drug candidate.

Table 4: ADME/screening for drug-likeness properties for compounds A1, B1, C1 and D1

	ADME PROPERTIES						
COMPOUND	mLogP	TPSA (Å)	MW	n-ON	n-OHNH	n-Voi	n-rotb
A1	-0.16	29.46	97.09	2	1	0	1
B1	-0.76	18.46	154.12	4	0	0	3
C1	-1.90	49.69	127.07	4	2	0	0
D1	-1.94	79.15	164.16	5	3	0	3

Key: Lipophilicity (mLogP), topological polar surface area (TPSA), molecular weight (MW), number of hydrogen bond acceptors (n-ON), number of hydrogen bond donors (n-OHNH), number of violated drug-likeness rules (n-Voi), number of rotable bonds (n-rotb)

5.0 Molecular docking

To affirm the ability of the affinity of the studied compounds, distinct proteins have

been studied using molecular docking performed with the aid of the Autodockvina software. Molecular docking is a computational model which shows the interaction between the ligand and the selected proteins and also estimates the binding affinities and conformance of the drug to the distinct proteins [27]. In attempt to find new drugs via molecular docking of the compounds within the active site of the inflammatory and nociceptive bacterial whichreveals their inhibitory efficiency, the proteins were downloaded from the PDB database (www.RSCPDB.org); E. callabus(4ZBR), O. cuniculus(1NR6). The preparations of these proteins were achieved using the discovery studio which is able to allocate modification in the deformity of amino acid sequence, include ionic hydrogen and charges to the protein molecule, removing the water molecule and making them suitable for the docking process.3D structure of the distinct receptor proteins is presented in Figure 4a-b.Structural optimizations were carried out for the ligands used for docking. This was done using the Gaussian09W software at B3LYP/6-311++g(d,p) for the complexes(A1, B1 and C1) and UB3PW91/6-311++g (2d,2p)meta hybrid GGA basis setsfor complex (D1). The ligandsbinds with the docking site of the receptor protein and interactions like Hydrogen bonding, unfavorable Donor-Donor bond, Pi-Anion, Pi-Sigma, Pi-Alkyl, Carbon Hydrogen bond and other interactions is seen inFigure4a-b.Visualization has also been made available using the Pymol software package and is presented in Figure 4a. The binding affinity of the compounds with the receptor proteins is seen in Table 5. The ligand B1 displayed maximum binding affinities of -5.8Kcal/moland -5.8Kcal/molwith the proteins 4ZBRand 1UR6 respectively. Similar binding affinity values were observed for other ligands with slight deviation ranging between 0.5 and 1.4. Ligand A1 had binding affinities of -4.4 Kcal/mol, and -4.5 Kcal/mol with the proteins 4ZBR and 1NR6 respectively; Ligand C1 had binding affinities of -5.3Kcal/moland -5.0 Kcal/mol with the proteins 4ZBR and 1NR6 respectively; Also, Ligand D1 had binding affinities of -5.3 Kcal/moland -4.5 Kcal/mol with the proteins 4ZBR and 1NR6 respectively.Apart from the binding affinity results, other interactions like the Hydrogen bond, pi-cation, pi-alkyl and others proved excellent on the active site of the receptor proteins with the ligands as seen in Figure 4a-b.From the results obtained, ligand B1 showed better inhibition potency for inflammation proteins than other ligands seeing that it had the highest binding affinity values in it interaction with both receptor proteins.

Table 5:Binding affinity results with amino acid residue of the ligands with the receptor proteins

PROTEIN	LIGAND A1		LIGAND B1		LIGAND C1		LIGAND D1	
	Binding Affinity (Kcal/mol)	Amino acid residue	Binding Affinity (Kcal/mol)	Amino acid residue	Binding Affinity (Kcal/mol)	Amino acid residue	Binding Affinity (Kcal/mol)	Amino acid residue
4ZBR	-4-4	TYR149, SER191, GLU291, ALA290, LYS194	-5.8	LEU406, LEU42, LEU452, ARG541, SER488, TYR410	-5.3	LEU429, LEU452,VAL 387	-5.3	LYS413, SER488, ARG484, TYR410
1NR6	-4.5	PRO424, GLN353, LEU358, THR298, ALA438	-5.8	GLN353, LEU358, THR302, ALA438, PHE425, THR298, THR299, ALA438	-5.0	THR298, THR299, THR302, ALA438, GLN353	-4.5	CYS432, ARG430, SER426, ARG97

Figure 4a: Pymol visualization of the ligands with the various receptor

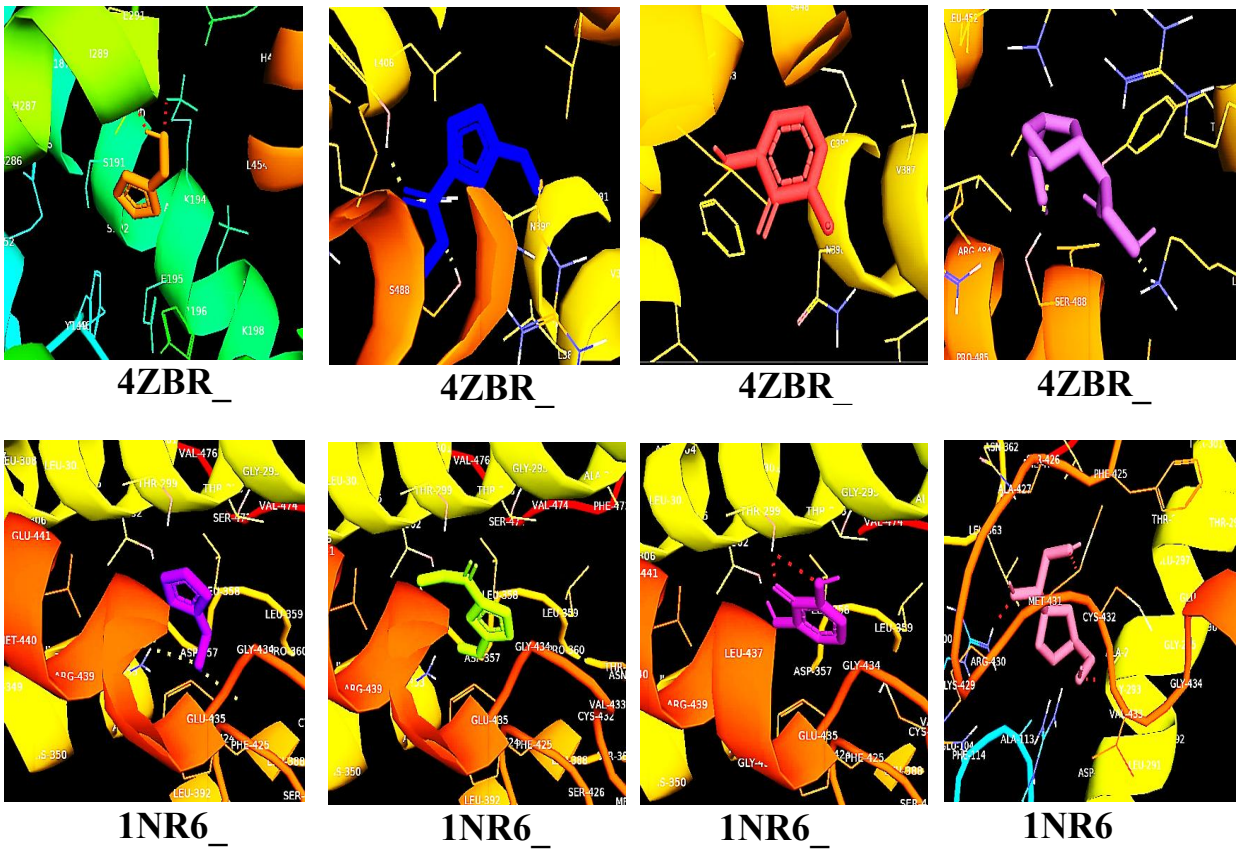

Conclusions

The HOMO-LUMO analysis showed complex A1 and B1 as a good anti-inflammatory and anti-nociceptive agent since they have the highest ionization potential values of 7.425eV and 7.4391eV. The energy gap which best describes the stability of a compound showed B1 to be the most stable since it possesses the least energy gap value 4.671eV. Natural bonding orbital analysis (NBO) which significantly reveals the contribution of the complex as calculated by the gas phase revealed that the interactions of the compounds were hyperconjugative in nature and the isolated compounds were stabilized mostly by the charge emanating from($\Delta ET\pi^* \rightarrow \pi^*$). The Mulliken population analysis explicitly depicts the atomic charges possessed by each atom and the effect of their functional groups on the charges had it that the charge density in C3 = –0.378 for complex B1 is higher than those observed for other complexes. The ADME (absorption, distribution, metabolism and excretion) parameters carried out on the compounds to

elucidate it drug-likeness ability were within the permissible limits. All compounds had zero violation (n-Voi),number of hydrogen bond donors (n-OHNH)< 5, number of hydrogen bond acceptors (n-ON) < 10, lipophilicity (mLogP) < 4.15 and molecular weight (MW) < 500 indicating good oral behaviors and excellent permeability factor of the compounds. Molecular docking proved excellent on the interactions of all ligands on the active site of the receptor proteins via the binding affinity values obtained: 4ZBR_A1 (-4-4 Kcal/mol), 4ZBR_B1 (-5.8 Kcal/mol), 4ZBR_C1(-5.3 Kcal/mol), 4ZBR_D1 (-5.3 Kcal/mol), 1NR6_A1 (-4.5 Kcal/mol), 1NR6_B1 (-5.8 Kcal/mol), 1NR6_C1 (-5.0Kcal/mol), 1NR6_D1 (-4.5 Kcal/mol) However, it showed a slightly distinctive potential on complex B1 as the best potential drug candidate for the case study among others seeing that it has the highest binding affinity value of (-5.8 Kcal/mol) in it interaction with both proteins.

Declaration of Competing Interest

The authors declare zero financial and inter-personal conflict of interest that could have influenced the research work and results reported in this research paper.

Acknowledgment: The authors are appreciative to TETfund for funding this research.

References

1. Serhan, C. N., Brain, S. D., Buckley, C. D., Gilroy, D. W., Haslett, C., O'Neill, L. A., ... & Wallace, J. L. (2007). Resolution of in flammation: State of the art, definitions and terms. The FASEB journal, 21(2), 325-332.
2. Merinen, M., Irjala, H., Salmi, M., Jaakkola, I., Hänninen, A., &Jalkanen, S. (2005). Vascular adhesion protein-1 is involved in both acute and chronic inflammation in the mouse. The American journal of pathology, 166(3), 793-800.
3. Belmonte, C., Nichols, J. J., Cox, S. M., Brock, J. A., Begley, C. G., Bereiter, D. A., ... &Wolffsohn, J. S. (2017). TFOS DEWS II pain and sensation report. The ocular surface, 15(3), 404-437.
4. Combe, R., Bramwell, S., & Field, M. J. (2004). The monosodium iodoacetate model of osteoarthritis: a model of chronic nociceptive pain in rats?. Neuroscience letters, 370(2-3), 236-240.
5. Steeds, C. E. (2009). The anatomy and physiology of pain. Surgery (Oxford), 27(12), 507-511.
6. Linley, J. E., Rose, K., Ooi, L., &Gamper, N. (2010). Understanding inflammatory pain: ion channels contributing to acute and chronic nociception. PflügersArchiv-European Journal of Physiology, 459(5), 657-669.
7. Calado, G. P., Lopes, A. J. O., Costa Junior, L. M., Lima, F. D. C. A., Silva, L. A., Pereira, W. S., ... &Nascimento, F. R. (2015). Chenopodiumambrosioides L. reduces synovial inflammation and pain in experimental osteoarthritis. PLoS One, 10(11), e0141886.

8. Muslu, H., Kalaycıoğlu, Z., Erdoğan, T., Gölcü, A., &Erim, F. B. (2021). Synthesis, characterization, anti-inflammatory evaluation, molecular docking and density functional theory studies of metal based drug candidate molecules of tenoxicam. Results in Chemistry, 3, 100111.

9. Obafemi, C. A., Adegbite, O. B., Fadare, O. A., Iwalewa, E. O., Omisore, N. O., Sanusi, K., ... &Ceylan, Ü. (2021). Tryptanthrin from microwave-assisted reduction of isatin using solid-state-supported sodium borohydride: DFT calculations, molecular docking and evaluation of its analgesic and anti-inflammatory activity. Heliyon, 7(1), e05756.

10. Steptoe, A., & Wardle, J. (2005). Cardiovascular stress responsivity, body mass and abdominal adiposity. International journal of obesity, 29(11), 1329-1337.

11. Jejurikar, B. L., &Rohane, S. H. (2021). Drug designing in discovery studio. Asian J Res Chem, 14(2), 135-138.

12. Zhurko, G. A., &Zhurko, D. A. (2009). ChemCraft, version 1.6. URL: http://www. chemcraftprog. com.

13. Hanwell, M. D., Curtis, D. E., Lonie, D. C., Vandermeersch, T., Zurek, E., & Hutchison, G. R. (2012). Avogadro: an advanced semantic chemical editor, visualization, and analysis platform. Journal of cheminformatics, 4(1), 1-17.

14. Monaco, G., Summa, F. F., &Zanasi, R. (2020). Program Package for the Calculation of Origin-Independent Electron Current Density and Derived Magnetic Properties in Molecular Systems. Journal of Chemical Information and Modeling, 61(1), 270-283.

15. Husain, A., Ahmad, A., Khan, S. A., Asif, M., Bhutani, R., & Al-Abbasi, F. A. (2016). Synthesis, molecular properties, toxicity and biological evaluation of some new substituted imidazolidine derivatives in search of potent anti-inflammatory agents. Saudi Pharmaceutical Journal, 24(1), 104-114.

16. Jejurikar, B. L., &Rohane, S. H. (2021). Drug designing in discovery studio. Asian J Res Chem, 14(2), 135-138. Pawar, S. S., &Rohane, S. H. (2021). Review on discovery studio: an important tool for molecular docking. Asian J. Res. Chem, 14, 86-88.

17. DeLano, W. L. (2002). Pymol: An open-source molecular graphics tool. CCP4 Newsl. Protein Crystallogr, 40(1), 82-92.

18. Nguyen, N. T., Nguyen, T. H., Pham, T. N. H., Huy, N. T., Bay, M. V., Pham, M. Q., ...& Ngo, S. T. (2019). Autodockvina adopts more accurate binding poses but autodock4 forms better binding affinity. Journal of Chemical Information and Modeling, 60(1), 204-211.

19. Salzner, U., & Baer, R. (2009). Koopmans' springs to life. The Journal of chemical physics, 131(23), 231101.

20. Bisong, E. A., Louis, H., Unimuke, T. O., Odey, J. O., Ubana, E. I., Edim, M. M., ... &Utsu, P. M. (2020). Vibrational, electronic, spectroscopic properties, and NBO analysis of p-xylene, 3, 6-difluoro-p-xylene, 3, 6-dichloro-p-xylene and 3, 6-dibromo-pxylene: DFT study. Heliyon, 6(12), e05783.

21. Louis, H., Gber, T. E., Asogwa, F. C., Eno, E. A., Unimuke, T. O., Bassey, V. M., &Ita, B. I. (2022). Understanding the lithiation mechanisms of pyrenetetrone-based carbonyl compound as cathode material for lithium-ion battery: Insight from first principle density functional theory. Materials Chemistry and Physics, 278, 125518.

22. Agwupuye, J. A., Louis, H., Unimuke, T. O., David, P., Ubana, E. I., &Moshood, Y. L. (2021). Electronic structure investigation of the stability, reactivity, NBO analysis, thermodynamics, and the nature of the interactions in methyl-substituted imidazolium-based ionic liquids. Journal of Molecular Liquids, 337, 116458.

23. Louis, H., Amodu, I. O., Unimuke, T. O., Gber, T. E., Isang, B. B., &Adeyinka, A. S. (2022). Modeling of Ca12O12, Mg12O12, and Al12N12 nanostructured materials as sensors for phosgene (Cl2CO). Materials Today Communications, 103946.

24. VÁZquez, J., & Stanton, J. F. (2006). Simple (r) algebraic equation for transition moments of fundamental transitions in vibrational second-order perturbation theory. Molecular Physics, 104(3), 377-388.

25. Paul, B. K., &Guchhait, N. (2011). TD–DFT investigation of the potential energy surface for Excited-State Intramolecular Proton Transfer (ESIPT) reaction of 10-hydroxybenzo [h] quinoline: Topological (AIM) and population (NBO) analysis of the intramolecular hydrogen bonding interaction. Journal of luminescence, 131(9), 1918-1926.

26. Lipinski, C. A. (2004). Lead-and drug-like compounds: the rule-of-five revolution. Drug discovery today: Technologies, 1(4), 337-341.

27. Eno, E. A., Patrick-Inezi, F. A., Louis, H., Gber, T. E., Unimuke, T. O., Agwamba, E. C., ...&Adalikwu, S. A. (2022). Theoretical investigation and antineoplastic potential of Zn (II) and Pd (II) Complexes of 6-Methylpyridine-2-carbaldehyde-N (4)-ethylthiosemicarbazone. Chemical Physics Impact, 100094.